

Supporting Information

Di Malta et al. 10.1073/pnas.1209577109

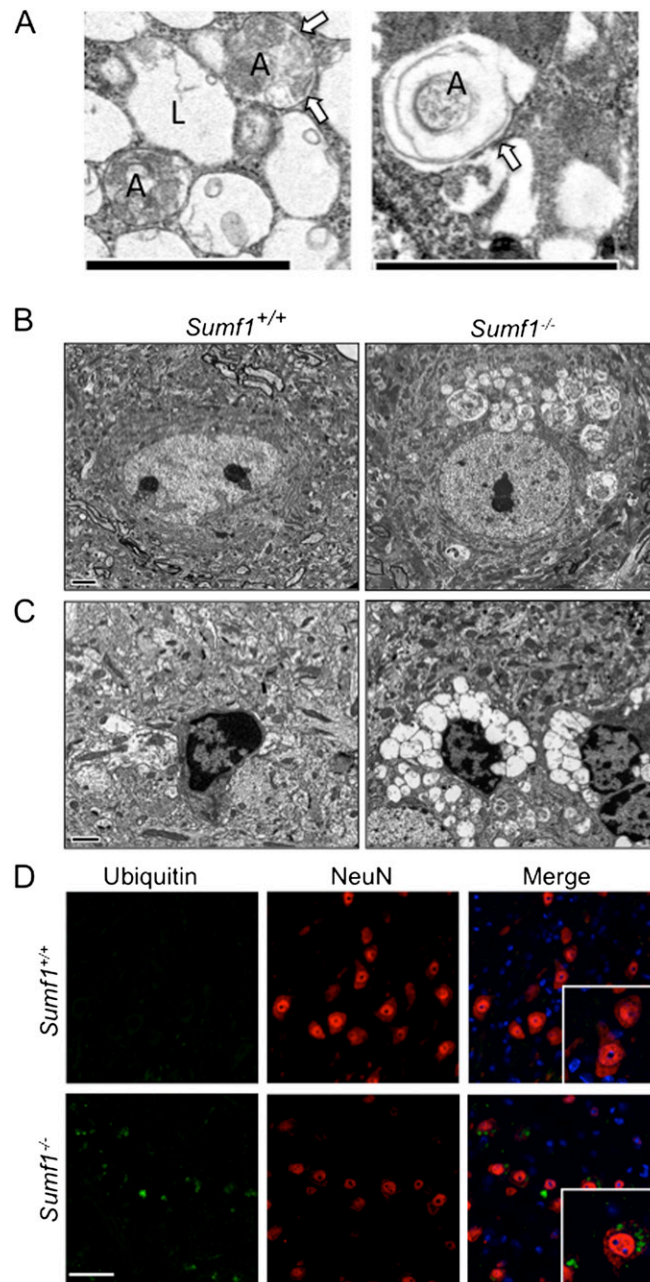


Fig. S1. Lysosomal and autophagic dysfunction in *Sumf1*^{-/-} neurons and glia. (A) Cytoplasmic vacuoles in *Sumf1*^{-/-} astrocytes. (Left) Autophagic vacuoles (A) surrounded by a double membrane (arrows) and containing electron-dense material resembling a portion of cytoplasm and lysosomal vacuoles (L) with clearer and more amorphous material. (Right) Autophagic vacuole surrounded by a double membrane (arrows). (B) Lysosomal storage in *Sumf1*^{-/-} neurons. Electron micrograph showing large vacuoles in the cytoplasm of neurons from a 3-mo-old *Sumf1*^{-/-} mouse (Right). Control neurons (Left) do not show signs of vacuolization. (C) Lysosomal storage in *Sumf1*^{-/-} microglia. Electron micrograph from the cortex of a 3-mo-old *Sumf1*^{-/-} mouse shows highly vacuolized microglia (Right). Microglia from a control mouse (Left) does not show signs of vacuolization. (D) Accumulation of ubiquitin-positive aggregates inside the cytoplasm of neurons. Brain tissue from 3-mo-old *Sumf1*^{-/-} and control mice immunostained with ubiquitin (green) and NeuN (red) antibodies. Insets show enlargement of the merge. (Scale bars: 2 μm in A and B; 1 μm in C; 10 μm in D.)

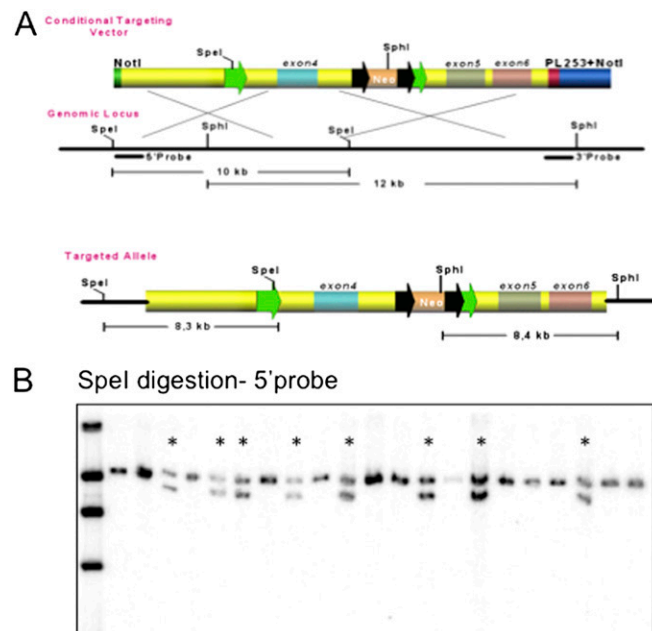


Fig. S2. Generation of *Sumf1* conditional-knockout mouse line. (A) Schematic representation of the homologous recombination event between the *Sumf1* targeting vector and the *Sumf1* genomic locus. Correctly targeted ES cells have an 8.3-kb SpeI-targeted band, in addition to a 10-kb wild-type band, following hybridization with the 5' probe. These clones also have an 8.4-kb SphI-targeted band, as well as a 12-kb wild-type band following hybridization with the 3' probe. (B) Germ-line transmission of the conditional allele. Genomic DNA derived from 21 pups was digested with SpeI, and the Southern blot was analyzed using the 5' probe; a total of eight germ-line mice were found (asterisks).

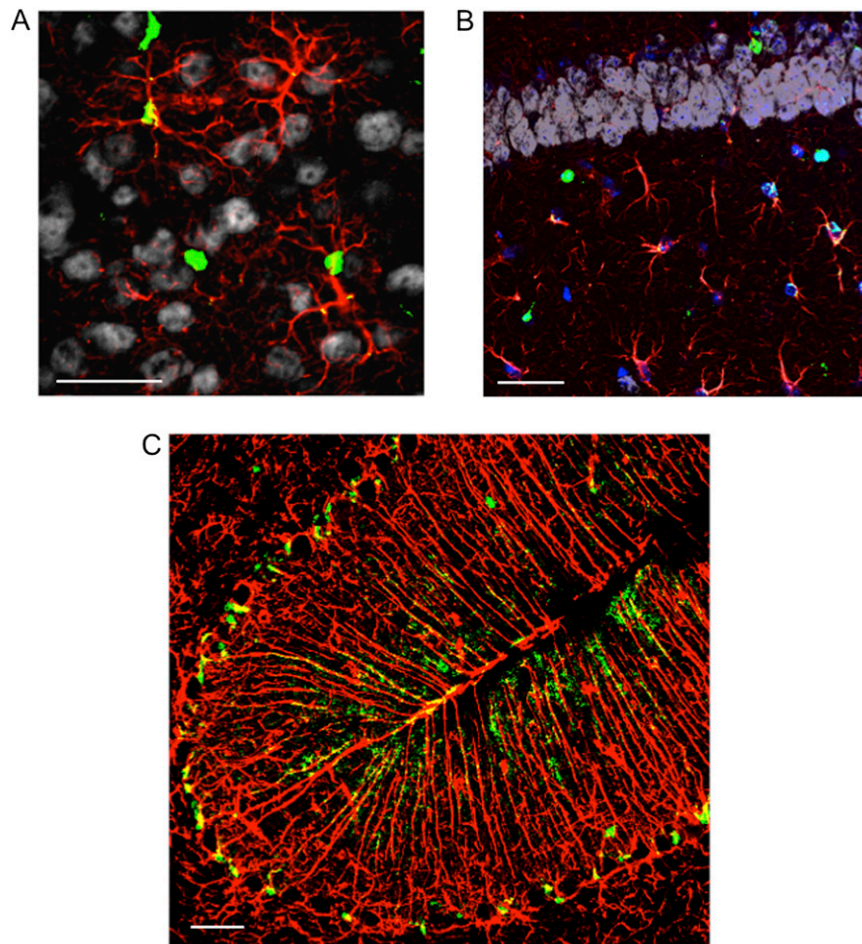


Fig. S3. Specificity of the GFAP-Cre transgenic line. (A and B) YFP protein colocalizes with the GFAP marker for astrocytes and not with the neuronal marker NeuN in the GFAP-Cre⁺; Rosa-YFP^{+/+} mouse. Immunostaining using GFP antibody (green), GFAP-antibody (red), and NeuN-antibody (gray) from cortex (A) and hippocampus (B). (C) Colocalization of YFP protein (green) with GFAP marker (red) in the Bergmann glia of cerebellum in an GFAP-Cre⁺; Rosa-YFP^{+/+} mouse. (Scale bars: 20 μ m.)

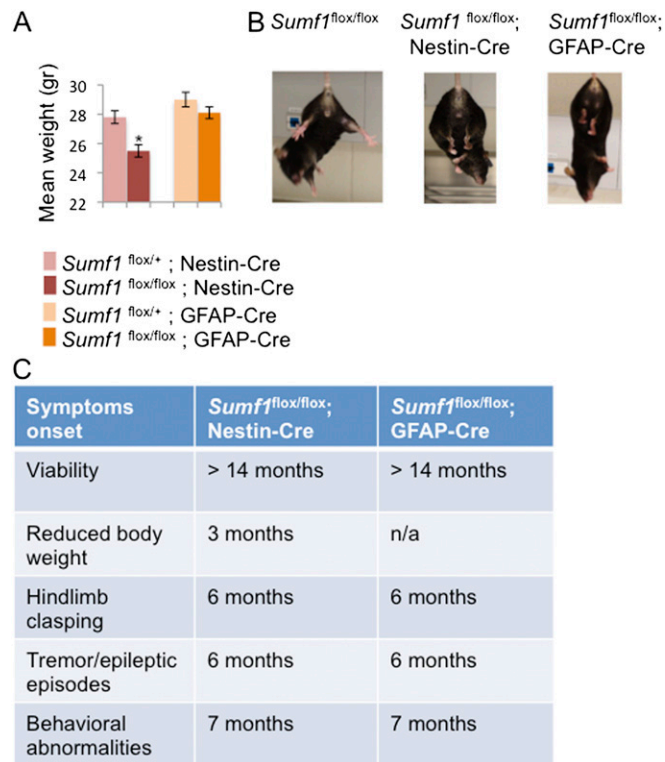


Fig. S4. *Sumf1*^{flox/flox}; Nestin-Cre and *Sumf1*^{flox/flox}; GFAP-Cre mouse phenotypes. (A) Weight loss in *Sumf1*^{flox/flox}; Nestin-Cre mice. Shown are mean weights of 3-mo-old mice of the indicated genotypes. Values represent mean \pm SEM of 10 mice for each group. * $P \leq 0.05$, Student's *t* test. (B) Abnormal limb-clasping reflexes in 6-mo-old *Sumf1*^{flox/flox}; Nestin-Cre and *Sumf1*^{flox/flox}; GFAP-Cre mice. (C) Summary of symptoms onset in *Sumf1*^{flox/flox}; Nestin-Cre and *Sumf1*^{flox/flox}; GFAP-Cre mice.

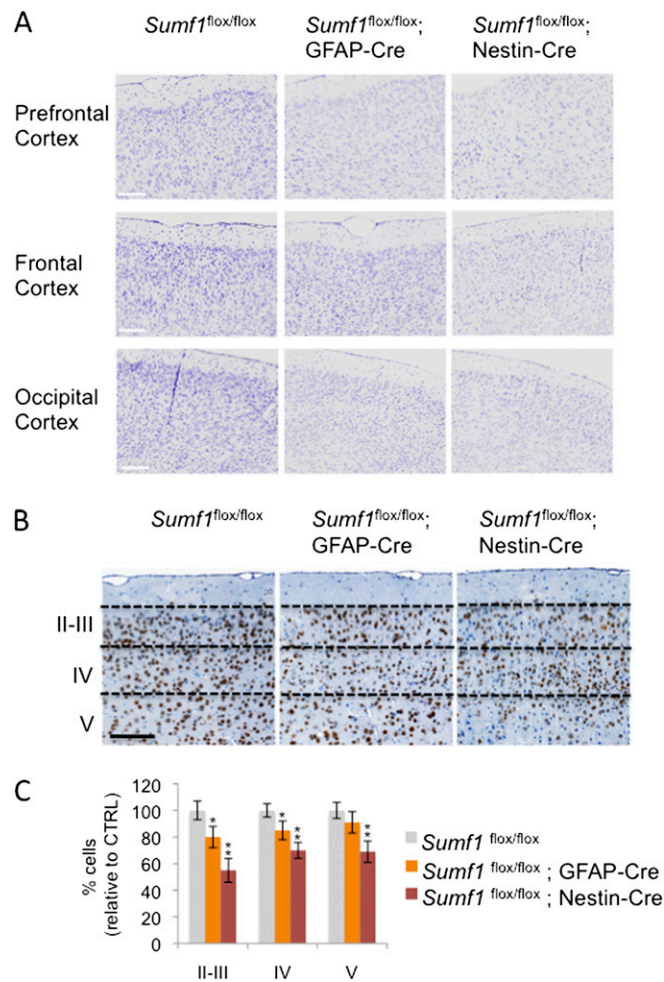


Fig. 55. Neurodegeneration in 6-mo-old *Sumf1*^{flox/flox}; GFAP-Cre and *Sumf1*^{flox/flox}; Nestin-Cre mice. (A) Nissl staining of brain slices from control (*Sumf1*^{flox/flox}), *Sumf1*^{flox/flox}; GFAP-Cre, and *Sumf1*^{flox/flox}; Nestin-Cre mice. Different areas of the cortex from each genotype are shown. (Scale bars: 200 μ m.) (B) NeuN immunostaining of frontal cortex sections from mice of the indicated genotypes. Dashed lines mark the different cortical layers. (C) Quantification of cortical neuron in *Sumf1*^{flox/flox}; Nestin-Cre and *Sumf1*^{flox/flox}; GFAP-Cre mice relative to control. The graph represents mean \pm SEM expressed as percentage relative to control. * $P \leq 0.05$, Student's *t* test. (Scale bars: 200 μ m.)

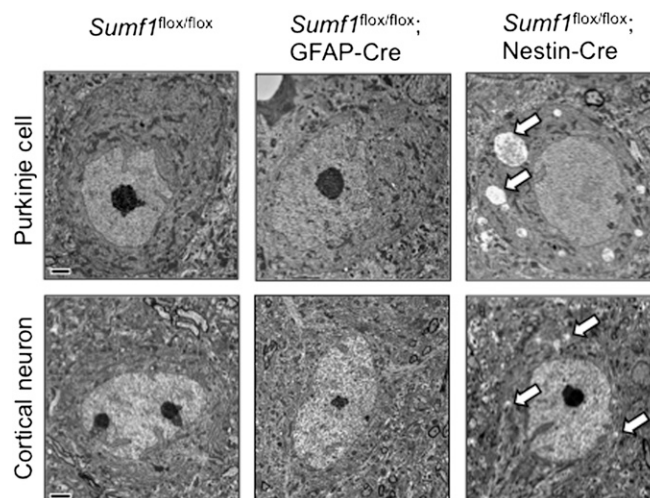


Fig. 56. Electron micrographs showing lysosomal storage in Purkinje cells (Upper) and cortical neurons (Lower) in brains from 3-mo-old *Sumf1*^{flox/flox}; Nestin-Cre, *Sumf1*^{flox/flox}; GFAP-Cre, and control mice. Vacuoles are evident only in neurons from *Sumf1*^{flox/flox}; Nestin-Cre mice, and the vacuoles in cortical neurons appear fewer and much smaller (arrows) than the ones observed in the Purkinje cells from the same mouse (arrows). (Scale bars: 2 μ m.)

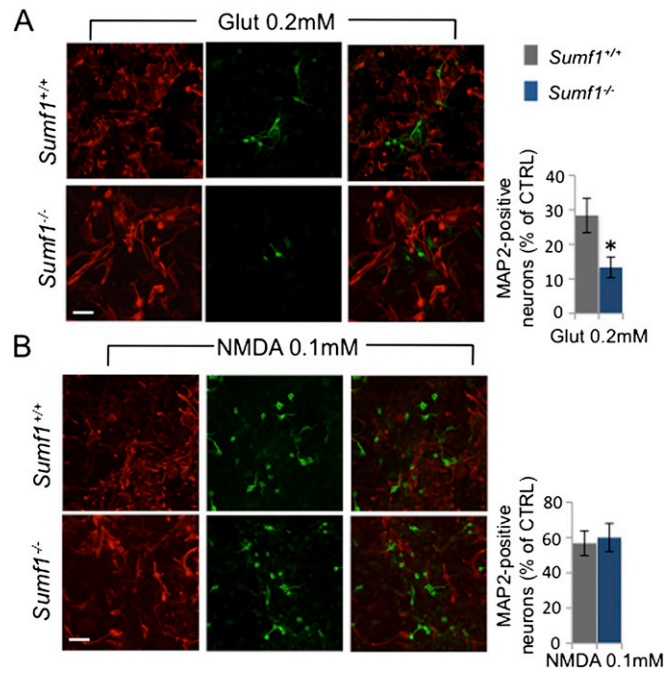


Fig. S7. *Sumf1^{-/-}* astrocytes fail to protect neurons against glutamate-mediated excitotoxicity. (A) MAP2 (green) and GFAP (red) immunostaining of neurons and astrocytes, respectively, showing that wild-type cortical neurons plated onto *Sumf1^{-/-}* cortical astrocytes are significantly less protected against glutamate-mediated excitotoxicity (0.2 mM for 24 h) than neurons plated on wild-type astrocytes (13 ± 3% in *Sumf1^{-/-}* vs. 28 ± 5% in wild type). (B) Stimulation with NMDA (0.1 mM for 24 h) did not alter survival of neurons grown on *Sumf1^{-/-}* astrocytes compared with neurons grown on wild-type astrocytes (60 ± 8% in *Sumf1^{-/-}* vs. 56 ± 7% in wild type). Histograms represent quantification of MAP2⁺ neurons after glutamate stimulation (A) and NMDA stimulation (B); the control is the correspondent sample without stimulation. Data represent mean ± SEM of three independent coculture experiments. **P* ≤ 0.05, Student's *t* test. (Scale bars: 20 μm.)

Neurological features	<i>Sumf1^{fllox/fllox}; Nestin-Cre</i>	<i>Sumf1^{fllox/fllox}; GFAP-Cre</i>
Hyperactivity	×	
Altered weight	×	
Hindlimb claspings	×	×
Motor incoordination	×	×
Motor learning	×	
Hypoactivity		×
Anxiety		×

Fig. S8. Summary of neurological features found in *Sumf1^{fllox/fllox}; Nestin-Cre* and *Sumf1^{fllox/fllox}; GFAP-Cre* mice. Comparison of the data obtained from the analysis of the two mouse models shows distinct behavioral phenotypes. "X" indicates the presence of the alterations in the specific lysosomal storage disorder neurological feature.